Journal of the Korean Physical Society, Vol. 56, No. 2, February 2010, pp. 562∼566

Observation of the Strong Negative Anomalous Hall Effect in Co-ion-implanted ZnO Single Crystals

Y. Y. Song, K. H. Park, K. S. Park, S. K. Oh and H. J. Kang*
Department of Physics, Chungbuk National University, Cheongju 361-763

D. S. Yang
Physics Division, School of Science Education, Chungbuk National University, Cheongju 361-763

S. W. Shin and J. H. Song
Korea Institute of Science and Technology, Seoul 136-761

(Received 12 May 2009, in final form 24 September 2009)

Eighty-keV Co ions with a dose of 3×10^{16} ions/cm^2 were implanted into high-quality 0.5-mm-thick ZnO (0001) single crystals with very low carrier concentration of n = 2.0×10^{13}/cm^3. The implanted samples were post-annealed at 700, 800, and 900 °C by rapid thermal annealing in a N_2 atmosphere. The structural, magnetic, and transport properties of Co-ion-implanted ZnO were investigated. The Co K-edge extended X-ray absorption fine structure analysis revealed the coexistence of Co-Co and Co-Zn bonds. The Co ions substituted into Zn sites form $Zn_{1-x}Co_xO$. Magnetoresistance (MR) data showed a sign change from positive to negative between 50 K and 77 K. A strong negative anomalous Hall effect (SNAHE) was observed in the temperature range with a positive MR. The sign change in the observed SNAHE seems to support the theory of Burkov and Balents.

PACS numbers: 75.50.Pp , 75.70.Ak , 72.20.M
Keywords: Diluted magnetic semiconductor, Anomalous Hall effect, Magnetoresistance, EXAFS, SQUID
DOI: 10.3938/jkps.56.562

I. INTRODUCTION

Recently, spin-based electronics (spintronics) [1]has attracted immense attention due to the possibility of using spin degrees of freedom charge carriers for future devices. Dilute magnetic semiconductors (DMS), for example II-VI ZnO [2–7] and III-V GaAs[8,9] doped with transition metals, have emerged as one of the potential candidates to develop such devices. Although Co- and Mn-doped ZnO were reported to have a high ferromagnetic transition temperature (T_c), some confusion remains as to its DMS nature [2–7].

If the DMS state is to be confirmed, it is essential to check the transport properties of spin polarized carriers. In turn, the anomalous Hall effect (AHE) turns out to be a key ingredient in confirming the DMS properties because the AHE is caused by strong spin-orbit coupling. Since the AHE contains an effect due to the sample magnetization, the Hall resistivity can be expressed in the form

$$\rho_H = R_0 B + R_s 4\pi M, \quad (1)$$

where R_0 is the ordinary Hall coefficient, and R_s is the anomalous Hall coefficient. The magnitude of R_s depends on the strength of spin-orbit coupling, and a sign change in R_s is affected by the magnetization and the direction of spin polarization. For example, if one assumes that the spin-polarized electron whose spins are parallel to the magnetization move to the right, they give rise to a positive AHE. Then, the spin-polarized electrons whose spins are antiparallel to the magnetization move to the left, they will give rise to a negative AHE.

Both the negative and the positive AHEs were observed in (GaMn)As [8,9]. This sign change in the (GaMn)As system may be understood through the theory of Burkov and Balents [10]. According to that theory, the anomalous Hall conductivity is proportional to the derivative of the density of states at the Fermi energy while the ordinary Hall conductivity is proportional to the density of states itself. As a result, the sign of the anomalous Hall conductivity can change when the Fermi level passes over the maximum of the impurity band. Several groups have observed the AHE in either Co- or Mn-doped ZnO films [2–6]. Most transition-metal-doped ZnO samples show a positive AHE coefficient, and the intensity of the AHE is mostly weak without the ordi-

*E-mail: hjkang@cbu.ac.kr; Fax: +82-43-274-4811

nary Hall term subtracted, owing to the weak coupling between the spin carrier and the localized electron. Very recently, Potzger *et al.* reported that high-dose Co-ion-implanted ZnO showed the existence of superparamagnetic clusters [7]. They also reported on the AHE, but reported a positive anomalous Hall coefficient. Therefore, investigating the aspect of the AHE phenomena in a ZnO structure doped with transition metal would be worth while.

Among semiconductor processing techniques, ion-implantation of transition metals into various semiconductors has been a powerful doping tool. In the present work, the structural, magnetic, and magneto-transport properties of high-quality ZnO single crystals implanted with cobalt ions were investigated. The magnetoresistance (MR) curve of this material showed a concave-down shape (positive MR) due to strong a s-d exchange interaction up to 50 K. A strong negative AHE was observed up to 50 K.

As indicated above, the sign change in R_s of the AHE term is proportional to the derivative of the density of states at the Fermi energy. As such, the sign change of the AHE term in our results provides a piece of evidence that supports the theory of Burkov and Balents [10]. Moreover, the strong anomalous Hall coefficient R_s observed here can provide DMS states at temperatures higher than 50 K.

II. EXPERIMENT

High-quality ZnO substrates with a very low carrier concentration n = 2.0 × 10^{13}/cm^3 at room temperature were used in this work. Eighty-keV Co ions with a dose of 3 × 10^{16} ions/cm^2 were implanted into 0.5-mm-thick ZnO (0001) single crystals at 350 °C. According to the SRIM code simulation, the projected range (R_p) of implanted Co ions was around 37 nm, and the maximum concentration near the R_p was about 8.4 at%. The implanted samples were post-annealed at 700, 800, and 900 °C by rapid thermal annealing (RTA) in a N_2 atmosphere for 5 min to recrystallize the samples and to remove implantation damage. Magnetization measurements were performed with a Quantum Design superconducting quantum interference device (SQUID). The extended X-ray absorption fine structure (EXAFS) measurements were performed by utilizing the synchrotron radiation from the 2.5 GeV storage ring at the beam line 3C1 of the Pohang Light Source in the Pohang Accelerator Laboratory, Korea. Co K-shell X-ray absorption spectra were obtained to determine the local structure surrounding the Co dopant. The magneto-transport properties were measured at various temperatures by using the van der Pauw technique. Fields up to 5T were applied at various temperatures.

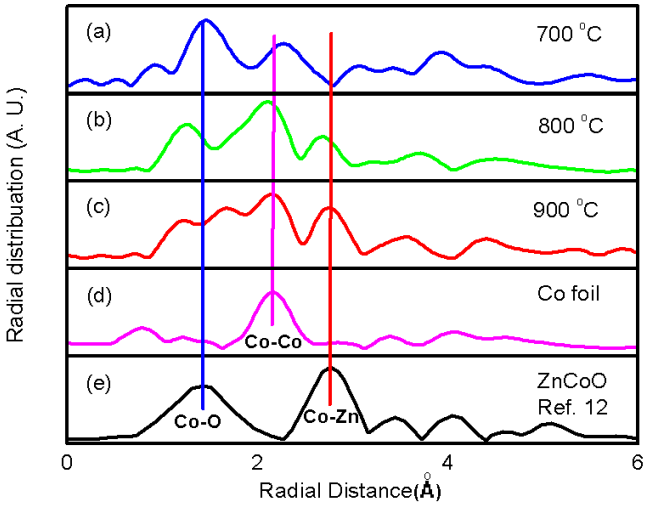

Fig. 1. Fourier transforms of Co K-edge EXAFS spectra of the Co-implanted ZnO for samples annealed at (a) 700 °C (b) 800 °C, and (c) 900 °C. Those for the (d) Co foil and the (e) $Zn_{1-x}Co_xO$:[Co] = 4.7% are from Ref. 12.

III. RESULTS AND DISCUSSION

The crystal structure of the Co-ion-implanted ZnO at various annealing temperatures was characterized by using high resolution X-ray diffraction (XRD) with standard θ-2(θ-2θ) scans and a Cu Kα source. The XRD data were reported in a previous paper [11]. The XRD diffraction peak shows an additional tiny peak corresponding to Co (111), which clearly indicates that Co particles are precipitated when the samples were annealed. The size of Co particles was obtained from the width of the Co (111) peak, which was measured by high resolution XRD via the Scherrer formula. The sizes of the Co precipitate were estimated to be 5.8 ± 0.9 and 8.7 ± 1.0 nm in the samples annealed at 800 °C and 900 °C respectively.

The bond structure of Co particles was investigated using EXAFS, from which we could obtain information related to the coordination environment of the central excited atom. In order to examine the local structure around the Co atoms, we obtained Co K-edge spectra for the samples post-annealed at 700 °C, 800 °C, and 900 °C. The spectrum of the Co metal foil was used as a reference. Figure 1 shows a series of Fourier-transformed Co K-edge EXAFS spectra for the samples post-annealed at 700 °C, 800 °C, and 900 °C. Those for Co metal foil and $Zn_{1-x}Co_xO$:[Co] = 4.7% are from Ref. 12. Each spectrum was processed by using the computer program IFEFFIT [13]. These three spectra for the samples annealed at 700, 800, and 900 °C show metallic Co-Co bonds. Here, the Co-Co bond indicates the existence of metallic clusters. There are two more bonds, *i.e.*, Co-O and Co-Zn. The intensity of those two peaks increases with increasing annealing temperature due to structure recovery. The Co-O and the Co-Zn bonds are thought to occur at Zn sites in $Zn_{1-x}Co_xO$, as indicated in Fig. 1(e)

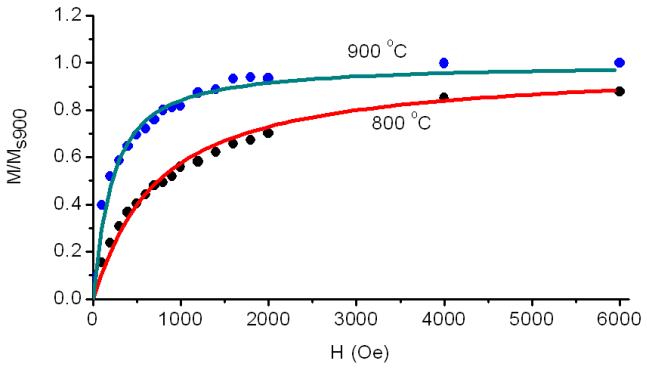

Fig. 2. Magnetic moment measured at 300 K by using a SQUID for the Co-implanted ZnO annealed at 800 and 900 °C. The solid lines represent the theoretical curves obtained by using the Langevin function.

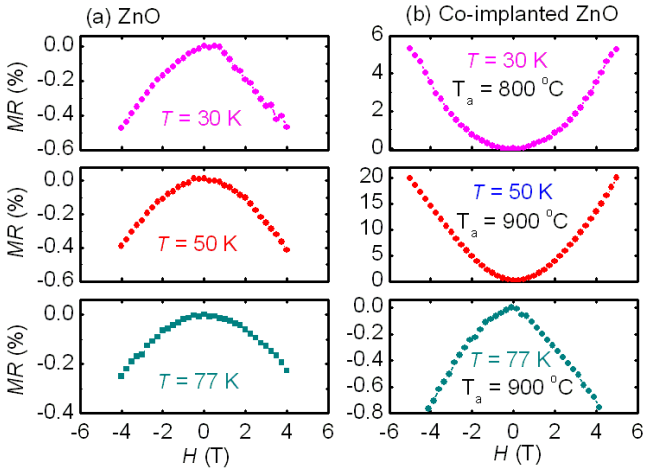

Fig. 3. MR(%) vs. static magnetic field H for (a) pure ZnO and (b) Co-implanted ZnO annealed at 800 and 900 °C. The measurment temperature is indicated.

[12]. These Co metallic clusters presumably yield results corresponding to the XRD results indicated above.

Nanometer-size Co precipitates can affect magnetization, which depends on the particle size. The magnetization was investigated using a SQUID for the samples annealed at 800 and 900 °C. The diamagnetic component from the ZnO substrate was subtracted. The magnetization curves of both samples at 5 K show clear ferromagnetic behaviors, having a larger ferromagnetic signal [11]. However, at room temperature, the ferromagnetic hysteresis of both samples disappears, within the resolution of the measurements. Instead, they showed a superparamagnetic behavior, hence, the coercivity and the remnant magnetization are zero. The magnetic moment was saturated at 6000 Oe in the sample annealed at 900 °C. The saturated magnetic moment was 4.95 $\times$ 10^{-5} emu. Considering the same number of Co ions in the films annealed at both 800 °C and 900 °C, the magnetic moment data can be normalized to the saturated magnetic moment of the sample annealed at 900 °C. Figure 2 shows representative room-temperature SQUID data on the induced M/M_{s900}vs. static field H, where M_{s900} indicates the saturated magnetic moment of the sample annealed at 900 °C. The solid circles in (a) and (b) are data for the samples annealed at 800 and 900 °C. Here, the magnetization of the sample annealed at 800 °C was not yet saturated at 6000 Oe, which is due to the smaller size of the Co particles compared to that of the Co particles annealed at 900 °C. The magnetization data for a superparamagnetic fine particle can be expressed by using the Langevin function as

$$\frac{M}{M_s} = \coth\{a(s)\} - \frac{1}{a(s)} \ , \qquad (2)$$

where, s is the particle size and $a(s) = \mu(s)H \ / \ k_BT$. In a real system, the particle size distribution should be taken into account in the equation, and the equation is given in Ref. 14 as

$$\frac{M}{M_s} = \int_0^\infty [\coth\{a(s)\} - \frac{1}{a(s)}]G(s - s_0)ds \ , \qquad (3)$$

where $G(s\text{-}s_0)$ is a Gaussian distribution, and s_0 is the mean particle size. By including the Gaussian distribution in Eq. (2), the data can be fitted with Eq. (3).

The solid line of Fig. 2 is a fit made with Eq. (3). The results give particle sizes of about 5.2 $\pm$ 1.5 nm and 7.8 $\pm$ 1.8 nm for the sample annealed at 800 and 900 °C, respectively. These values are quite similar to the XRD results within error bars. The number of Co ions included in the Co clusters is obtained from the saturated magnetization value of the sample annealed at 900 °C. It is estimated to be around 1.24 $\times$ 10^{16} atoms, which is about 40% of total number of implanted Co ions. There was no CoO peak in the XRD data obtained by using high-resolution XRD standard θ-2θ scans while the EXAFS spectra show a Co-O bond structure. These results reveal that 60% of the Co ions, apart from 40% of the Co clusters, could form the $Zn_{1-x}Co_xO$ compound. Considering that 60% of the Co ion substitute into Zn sites, the maximum amount, 8.4%, of Co obtained from the SRIM code simulation at R_p, as shown above, gives rise to $Zn_{0.9}Co_{0.1}O$. The difference in the saturation magnetization between 5 and 300 K is around 8.6 $\times$ 10^{-5} emu. We believe that the magnetization difference mainly come from $Zn_{0.9}Co_{0.1}O$ at 5 K and gives about 0.53 μ_B/ Co atom.

Although the films show clear evidence of superparamagnetism due to Co clusters at room temperature, the 60% of the Co ions that substitute into the Zn sites can affect the transport properties, revealing the interaction between the magnetization and the spin carriers. The magneto-transport measurements were carried out at temperatures ranging from 5 to 77 K. Figure 3 shows MR (%), defined by $[MR(H) - MR(0)] \ / \ MR(0)$, vs. the

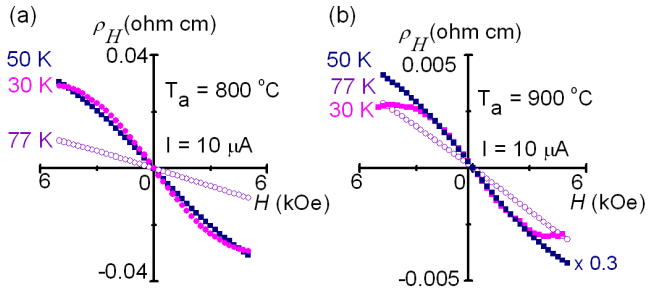

Fig. 4. Hall resistivity vs. magnetic field for Co-implanted ZnO annealed at (a) 800 and (b) 900 °C. All data in both graphs show raw data without the ordinary Hall term subtracted. The 50-K data in (b) are multiplied by 0.3.

applied magnetic field H for (a) pure ZnO and (b) for samples annealed at 800 and 900 °C. The *MR* of the pure ZnO sample shown in (a) gives a concave -down shape (negative *MR*) through the temperature range from 30 to 77 K. A similar behavior was observed in pure ZnO recently [15] and was caused by a shortage in the s-d exchange interaction. However, the two curves measured at 30 and 50 K for the samples annealed at 800 and 900 °C have opposite concavities while the curve measured at 77 K for the sample annealed at 900 °C shows the same concavity as the pure ZnO structure. Xu *et al.* [2] reported a sign change in the *MR* for Co-doped ZnO near n_c where the metal-insulator transition occurs. The opposite concavities at low temperatures, and high temperatures in Fig 3(b) may be due to a state variation from localized states at temperatures below 50 K to delocalized states at temperatures above 77 K with increasing temperature.

The magnetic properties are mainly due to Co clusters, and they show superparamagnetism at 300 K, mentioned above. However, by taking into account the Co-O and the Co-Zn bonds from EXAFS spectra and the 60% of Co ions substituted into ZnO samples, as AHE could appear in $Zn_{1-x}Co_xO$. Figure 4 shows the Hall resistivity as a function of the static magnetic field in Co-implanted ZnO post-annealed at 800 and 900 °C respectively. The fact that the Hall resistivity at 77 K decreases linearly with increasing static magnetic field in both graphs indicates that the normal carrier is the electron. The AHE was clearly observed and is strong in the samples both at 30 and 50 K even though the linear ordinary Hall term was not subtracted. The Hall data measured at 30 K, Fig. 4(b), shows a very strong AHE, and there is no contribution from the ordinary Hall term. The anomalous Hall term is conventionally attributed to asymmetric scattering processes involving a coupling between the electron carrier and the magnetic moment, so the strong anomalous Hall coefficient indicates a strong interaction between the electron carries and the magnetic moment. This effect can give rise to a DMS state at temperatures higher than 50 K while some previous reports on the Co-doped ZnO indicate a DMS state in the low temperature range of 10 – 20 K with a very weak signal [2,3]. More specifically, the AHE coefficients are negative in both samples at temperatures below 77 K, indicating that the AHE carrier is of an electron type. This behavior is very exciting considering that the MR is similar to that of Co-doped ZnO and that most transition-metal-doped ZnO shows a positive AHE, as indicated above. The theory of Burkov and Balents was developed for GaMnAs to explain the sign change in the AHE coefficient. However, it may be valid for ZnO as well when the Fermi energy passes over the impurity band maximum. This behavior may come from a different band structure in Co ion-implanted ZnO here compared to the band structure in Co-doped ZnO films near the impurity band.

IV. CONCLUSIONS

In this work, the structural, magnetic, and transport properties of Co-ion-implanted ZnO single crystals with post-annealing were investigated. EXAFS studies showed that our Co-ion-implanted ZnO samples contained both Co metallic clusters and Co ions. The Co metallic clusters contributed to the superparamagnetism. The Co ions substituted into Zn sites and contributed to forming $Zn_{1-x}Co_xO$. MR data showed a sign change from positive to negative, which is similar to the behavior manifested by Co-doped ZnO [2]. Even though superparamagnetism was observed for Co-ion-implanted ZnO single crystals, Co ion-implanted ZnO films showed a strong negative AHE coming from $Zn_{1-x}Co_xO$. The strong anomalous Hall coefficient can give a DMS state at a temperature beyond 50 K. Finally, the negative AHE seems to support Burkov and Balents's theory, where the sign of AHE depends on the derivative of the density of states at the Fermi energy.

ACKNOWLEDGMENTS

This work was supported by the Korea Science and Engineering Foundation (KOSEF-R01-2004-000-10882-0). The EXAFS measurement was performed at the 3C1 EXAFS beam line under the approval of the Pohang Accelerator Laboratory (No. 2005-2035-03).

REFERENCES

[1] S. A. Wolf, D. D. Awschalom, R. A. Buhrman, J. M. Daughton, S. von Molnár, M. L. Roukes, A. Y. Chtchelkanova and D. M. Treger, Science **294**, 1488 (2001).

[2] Q. Xu, L. Hartmann, H. Schmidt, H. Hochmuth, M. Lorenz, R. Schmidt-Grund, C. Sturm, D. Spemann and M. Grundmann, Phys. Rev. B **73**, 205342-1 (2006).

[3] S. J. Pearton, D. P. Norton, M. P. Ivill, A. F. Hebard, J. M. Zavada, W. M. Chen and I. A. Buyanova, IEEE Trans. Electron Dev., **54** 1040 (2007).
[4] Q. Xu, H. Schmidt, L. Hartmann, H. Hochmuth, M. Lorenz, A. Setzer, P. Esquinazi, C. Meinecke and M. Grundmann, Appl. Phys. Lett. **91**, 092503 (2007).
[5] W. Shim, K. Lee and W Lee, J. Appl. Phys. **101**, 123908-1 (2007). **93**,142507(2008)
[6] H. S. Hsu, C. P. Lin, H. Chou and J. C. A. Huang, Appl. Phys. Lett. **93**, 142507(2008).
[7] K. Potzger, S. Zhou, Q. Xu, A. Shalimov, R. Groetzschel, H. Schmidt, A. Mücklich, M. Helm and J. Fassbender, Appl. Phys. Lett. **93**, 232504 (2008).
[8] W. Allen, E. G. Gwinn, T. C. Kreutz and A. C. Gossard, Phys. Rev. B **70**, 125320-1 (2004).
[9] Y. Iye, A. Oiwa, A. Endo, S. Katsumoto, F. Matsukura, A. Shen, H. Ohno and H. Munekata, Mater. Sci. Eng. B **63**, 88 (1999).
[10] A. A. Burkov and L. Balents, Phys. Rev. Lett. **91**, 057202-1 (2003).
[11] W. Kim, H. J. Kang, S. K. Oh, Y. H. Cho, D. S. Yang, J. H. Lee, J. H. Song, S. K. Noh, S. J. Oh, C. S Kim, S. W. Shin and C. N. Whang, J. Korean Phys. Soc. **49**, 979 (2006).
[12] Martínez-Criado, A. Segura, J. A. Sans, A. Homs, J. Pellicer-Porres and J. Susini, Appl. Phys. Lett. **89**, 061906 (2006).
[13] M. Newville, J. Synchrotron Rad. **8**, 96 (2001).
[14] G. Xiao and C. L. Chien, J. Appl. Phys. **61**, 3308 (1987).
[15] Q. Xu, H. Schmidt, S. Zhou, K. Potzger, M. Helm, H. Hochmuth, M. Lorenz, A. Setzer, P. Esquinazi, C. Meinecke and M. Grundmann, Appl. Phys. Lett. **92**, 082508 (2008).